# Chapter 4

## Elevated phosphodiester and T2 levels can be measured in the absence of fat infiltration in Duchenne muscular dystrophy patients

M.T. Hooijmans, E.H. Niks, J. Burakiewicz, J.J.G.M Verschuuren, A.G. Webb, H.E. Kan

*NMR Biomed. 2017 Jan;30(1). doi: 10.1002/nbm.3667.*

## Abstract

Quantitative MRI and MRS are increasingly important as non-invasive outcome measures in therapy development for Duchenne muscular dystrophy (DMD). Many studies have focussed on individual measures such as fat fraction and metabolite levels in relation to age and functionality, but much less attention has been given to how these indices relate to each other. Here, we assessed spatially-resolved metabolic changes in leg muscles of DMD patients, and classified muscles according to the degree of fat replacement compared to healthy controls. Quantitative MRI (3-point Dixon and multi-spin echo without fat suppression and a tri-exponential fit) and 2D-CSI $^{31}$P MRS scans were obtained from eighteen DMD patients and twelve healthy controls using a 3T and a 7T MR scanner. Metabolite levels, $T_2$ values and fat fraction were individually assessed for five lower leg muscles. In muscles with extensive fat replacement, phosphodiester over ATP (PDE/ATP) inorganic phosphate over phosphocreatine (Pi/PCr), intracellular tissue pH and $T_2$ were significantly increased compared to healthy controls. In contrast, in muscles without extensive fat replacement, only PDE/ATP and $T_2$ values were significantly elevated. Overall, our results show that PDE levels and $T_2$ values increase prior to the occurrence of fat replacement and remain elevated in later stages of the disease. This suggests that these individual measures could not only function as early markers for muscle damage but also reflect potentially reversible pathology in the more advanced stages.

## Introduction

Duchenne Muscular Dystrophy (DMD) is an X-linked disease caused by a mutation in the DMD-gene, affecting approximately 1 in 3500 male new-borns. [1] The absence of a functional dystrophin protein in the muscle cells of DMD patients manifests itself in progressive muscle weakness, functional loss, and cardiac and respiratory failure. [2] Within muscle tissue different pathophysiological events, such as changes in energy metabolism, fat infiltration, oedema and fibrosis, take place simultaneously. [3] The time course of these various processes is not fully understood but it appears that initial inflammation, and changes in energy metabolism, are eventually followed by the replacement of muscle tissue by fat and fibrotic tissue. It is generally thought that fat replacement of muscle tissue is irreversible while other processes may be at least partially reversible.



Both MRI and MRS have been used to non-invasively map these individual pathophysiological processes in DMD. [4-7] Muscle replacement by fat is commonly determined by chemical shift based methods such as Dixon. This replacement correlates well with age, disease progression and functional measures. [8-11] Another MR parameter which is frequently used in DMD is the $T_2$, which reflects both fat replacement and inflammation/edema. If used without correcting for the presence of fat, these relaxation times are referred to as global $T_2$ values and display the same progressive course as the fat fraction. [12-14] In addition, it is possible to assess the individual $T_2$ relaxation times of fat and water. The water $T_2$ is thought to represent the inflammation component, and is elevated compared to healthy controls. [4, 15-17] In contrast to global $T_2$ values, water $T_2$ values decrease with age and disease progression, most likely inversely related to the increase of fibrotic tissue. [18] Finally, metabolic changes in the muscles of DMD patients can be detected by using phosphorous spectroscopy ($^{31}$P-MRS). Reduced phosphocreatine (PCr) levels which have been associated with loss of metabolic activity, elevated phosphodiester levels (PDE) which might be directed related to membrane anomalies and a more alkaline pH associated with leaky myocytes have been detected in DMD patients compared to healthy controls. [6, 19-22] Furthermore, the PCr over inorganic phosphate (Pi) ratio has been shown to decline with age while the PDE/ATP ratio increased with age. [22, 23] Until now most MR studies have focussed on individual MR parameters, and little attention has been given to how these indices relate to each other. In particular, the temporal relation between changes in metabolic parameters, obtained from $^{31}$P MRS, and changes in fat fraction and water $T_2$ assessed with quantitative MRI is unclear. In Becker Muscular Dystrophy (BMD) structural changes such as the replacement of muscle tissue by fat and fibrosis are predominantly present in later stages of

the disease, while metabolic changes occur earlier. [24] This suggests that metabolic changes precede fat replacement. In contrast, work in facioscapulohumeral dystrophy (FSHD) patients showed that metabolic changes were only present in muscles with extensive fat replacement, which suggests that in this muscular dystrophy, metabolic changes and fat replacement occur simultaneously. [25] Finally, recent work in the arm muscles of DMD patients indicated a linear relation between fat fraction and disease progression, while metabolic changes most likely show non-linear behaviour. [26] Taken together, this body of work highlights the fact that it is important to assess more than just one aspect of muscle damage in DMD for a better understanding of the time course of the pathophysiology. In order to do this, it is essential that different measures be spatially co-localized in order to compare the results. However, $^{31}$P MRS in DMD is commonly performed using surface coil localization, which makes it difficult to combine the results from spatially-resolved proton imaging and non-spatially-resolved MRS. The availability of higher field strength magnets creates the possibility to obtain high quality and muscle specific $^{31}$P MRS data within reasonable measuring times.

In this work, we present combined quantitative MRI and spatially-resolved (2D-CSI) $^{31}$P MRS data of the leg muscles in DMD patients to determine metabolic changes and inflammation in muscles with and without fat infiltration to assess if metabolic changes and inflammation vary in different stages of the disease process.

## Methods

### *Study population*

Eighteen DMD patients (Age: 9.2± 3.7 yrs.; range: 5-16 yrs) and twelve age matched healthy control subjects (Age: 9.7± 2.9 yrs.; range: 5-14 yrs) participated in this study. All healthy subjects were recruited from local schools and sport clubs, while all patients were recruited from the Dutch Dystrophinopathy Database. [27] All DMD diagnoses were confirmed by genetic testing. Fourteen DMD patients were ambulant, and four patients were wheelchair-bound. All patients used corticosteroids with intermittent dosing regimens, which varied between 8-10 days on/off. The local medical ethical committee approved the study and all subjects and/or their parents signed informed consent.

### *MR Examination*

All $^{31}$P datasets were acquired on a Philips 7T Achieva MR system (Philips Healthcare, The Netherlands) with a custom-built double-tuned birdcage coil. Patients were

positioned in a supine position, feet first in the scanner. The coil was positioned around the left lower leg, at the thickest part of the calf directly distal to the patella. The imaging protocol contained a gradient echo FISP sequence for anatomical imaging (15 slices; slice thickness 7mm; interslice gap 0.5 mm; repetition time (TR) 10 ms; echo time (TE) 3.0 ms; flip angle (FA) 30°; FOV 180x200 mm), a B0-map for shimming (14 slices; slice thickness 8 mm, no slice gap; TR/TE 30/3.11ms; FA 20°; FOV 160x180 mm) and a 2D phosphorous MRS Chemical Shift Imaging (CSI) dataset to assess skeletal muscle energy metabolism (FOV 200x200/150x150 mm; matrix size 10 x 10; TR 2000 ms; samples 2048; FA 45°; Hamming weighted acquisition with 12 signal averages at the central k-lines). No slice selection was applied. $^{31}$P data were measured over the entire length of the coil which covered 12 cm of the leg in the feet/head direction. Second order shimming was applied with an image based shimming routine. The 2D-CSI positioning was guided by the anatomical images. As the diameter of the lower leg and the boundaries between the different muscle groups change along the length of the leg, the 2D-CSI sequence was planned in such a way that within the volume of the coil a specific voxel was located within one individual lower-leg muscle. [24]



On the same day, quantitative imaging datasets were acquired at 3 Tesla. A 3-point gradient echo Dixon sequence was acquired of the same leg on a Philips 3T Ingenia MR system for fat quantification in the lower leg (23 slices; slice thickness 10 mm; interslice gap 5 mm; TR/TE/ΔTE 210/4.41/0.76 ms; NSA 2; FA 8°; FOV 180x180 mm). In addition, a multi turbo spin echo sequence (MSE) was acquired to determine the T2 (17 echoes; TR/TE/ΔTE 3000/8/8 ms; echo train (8-136ms); voxel size 1.4x1.8x10 mm; gap 20 mm; slice thickness 10 mm; 5 slices, no fat suppression, refocussing pulse shape: central part of a sinc function , CPMG condition). The middle of the slice stack was positioned on the thickest part of the calf directly distal to the patella, to ensure accurate co-localisation with the $^{31}$P data set.

## Data-analysis

All phosphorous data sets were visualized with the 3D Chemical shift imaging package (3DiCSI). Individual spectra were identified in 5 lower leg muscles; the lateral (GL) and medial (GM) head of the gastrocnemius muscle, the soleus muscle (SOL), tibial anterior muscle (TA) and peroneus (PER) muscle with a grid overlay on the anatomical image. Voxels were carefully positioned to avoid overlap with adjoining muscles. All individual free induction decays were exported and processed with AMARES in jMRUI software package (version 5, http://sermn02.uab.es/mrui/). [28] Signals of Pi, PDE, PCr and γ-, α- and β-ATP were fitted with Gaussian line shapes. All metabolites are presented as a ratio over γ-ATP signal. Metabolite ratios were

corrected for partial saturation using literature values. [29] In addition, prior knowledge on the line width, as described previously, was used for PDE and β-ATP.[24] To calculate intracellular tissue pH, the shift in resonance between the Pi peak and PCr peak was used: pH=6.75 + log((3.27-S)/(S-5.69)). [30] As the disease progression in DMD patients is characterized by replacement of muscle tissue with fat, spectra of several patients suffered from a low signal-to-noise ratio (SNR) due to the low amount of muscle tissue in the voxel. To ensure spectral quality, SNR values were determined for each spectrum. Noise was defined as the standard deviation of the residual signal after the fitting procedure. Only spectra with SNR greater than 10 for the PCr peak in combination with the ability to properly fit all other metabolites were accepted.

Quantitative fat fractions were generated from 3-point Dixon images using (SI) fat/(SI fat+ SI proton))*100 according to a multi peak model containing six peaks. [31] As the sequence was optimized with respect to TR and FA for minimization of T1 relaxation effects, no correction for different T1 values was needed.[32] The sequence was not corrected for $T_2$* relaxation. [33, 34]

T2 values were calculated from the MSE images according a tri-exponential fitting routine written in Matlab (Mathworks, Natick, MA, USA) based on a previously described method. [35] The assumed $T_2$ fat values part of the tri-exponential fitting model were individually determined for each of the datasets. No $B_1^+$ sorting was applied, as $B1^+$ maps were analysed and almost all voxels fell within the general rejection criteria set for $T_2$ quantification ($B1^+$ lies in the range of 80-130% of the nominal $B1^+$ set by the scanner) Regions of interest (ROI) were drawn for the five individual lower leg muscles on all the slices within the coverage of the 2D-CSI using Medical Image Processing Analysis and Visualization (MIPAV) software (http://mipav.cit.nih.gov). T2 and fat fraction are presented as a mean value of all pixels within a ROI over multiple slices. All muscles of DMD patients were classified into two groups according to their fat fractions: Non-fat-infiltrated (NFI) DMD patients and fat-infiltrated DMD patients (FI DMD). Cut-off levels were determined for each muscle individually, using the mean fat fraction + 2* SD of that specific muscle in HC subjects.

### *Statistical analysis*

A general linear model was used to compare Pi, PCr, PDE, ATP and pH and T2 levels between groups for the five lower leg muscles. Age was entered as a covariate. Statistical analyses were performed in SPSS version 20 for Windows (SPSS Inc., Chicago) and the level of statistical significance was corrected for multiple testing and set at ($p<0.002$). After which a post-hoc analysis was used to assess which groups

(HC subjects, NFI and FI DMD patients) were different. Fischer's Least Significant Difference (LSD) model was used to correct for multiple comparisons during post-hoc analysis, significance level was set at ($p<0.05$).

## Results

Reconstructed T2 maps and corresponding fit of one of the voxel of the three analysed slices are visualized in Figure 1. Examples of 3T images and $^{31}P$ spectra of a non-fat infiltrated DMD patient, a fat infiltrated DMD patient and a healthy control subject are depicted in Figure 2. For the healthy controls, all the spectra reached the quality control criteria. For the DMD patients, 16 out of 90 spectra had to be excluded due to lack of sufficient quality (GL=6/18; GM 4/18; SOL= 1/18; TA=3/22; PER=2/18).



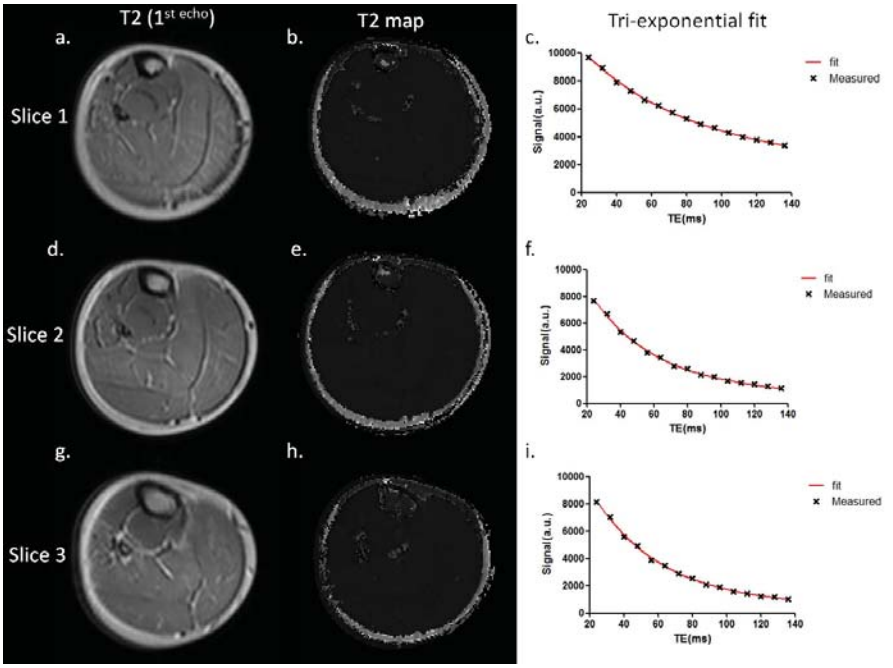


**Figure 1.** Axial multi-spin echo images of the right lower leg of a non-fat infiltrated DMD patient showing the 1st echo (TE: 8ms) of the three inner slices (a,d,g); the reconstructed T2 map of those three slices (b,e,h); and the corresponding fit of a single point located in the Soleus muscle for those three slices (c,f,i). the measured signal is shown using black crosses and the fitted signal using the red line. The first two echoes (not shown) were not used for the fit to eliminate potential influence of stimulated echoes. TE = echo timo (ms) and a.u. are arbitrary units.

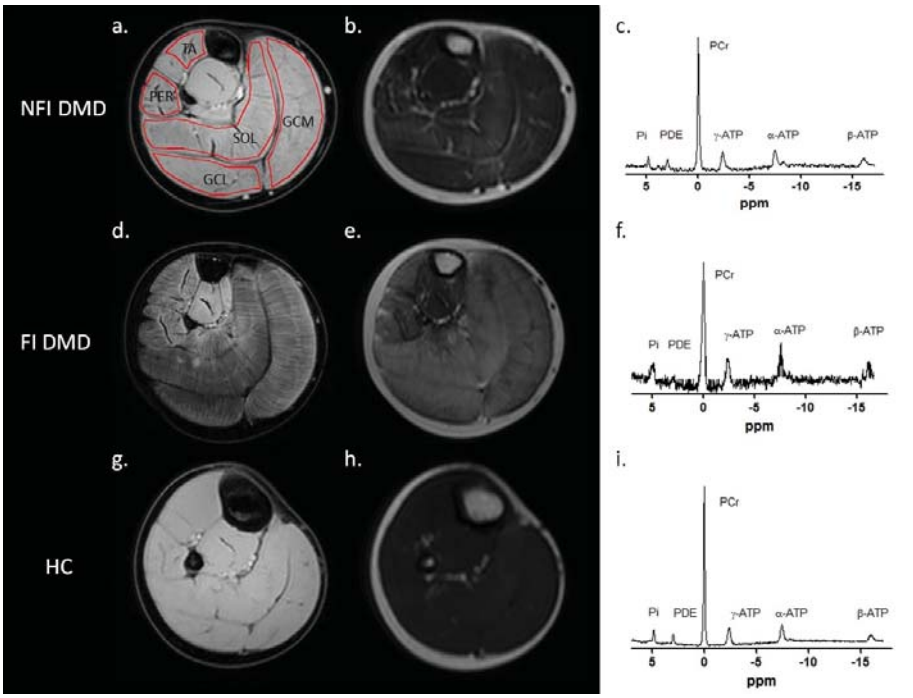


**Figure 2.** Axial images of the right lower leg of a FI DMD patient (a-c), NFI DMD patient (d-f) and a HC subject(g-i): (a, d, g);(a) proton images with a representation of the manually drawn ROIs for the five lower leg muscles - medial and lateral head of gastrocnemius (GM, GL), soleus (SOL), anterior tibialis (TA) and the peroneus (PER) muscles. (b, e, h); the 7$^{th}$ echo of a multi-spin-echo image (TE: 56 ms);(c, f, i) a representative $^{31}$P spectrum for a FI DMD patient [c] NFI DMD patient [f] and a healthy control subject [i]. Note the reduction in SNR in the phosphorous spectrum of the DMD patient.

### *Metabolite ratios classified according to fat fraction*

For the analysed muscles the NFI/FI DMD subgroups were divided as follows; GL NFI n=5/ FI n=7 (cut-off fat fraction 11.37%), GM NFI n=6/ FI n=8 (cut-off 10.05%), PER NFI n=4/ FI n=12 (cut-off 12.62%), SOL NFI n=7/ FI n=11 (cut-off 9.64%), TA NFI n=7/ FI n=8 (cut-off 10.81%). Metabolite ratios, $T_2$ values and fat fractions for the healthy controls and NFI and FI DMD patients are shown in the supplemental data (Table.1). Compared to healthy controls, PDE/ATP levels were significantly increased in the NFI and FI DMD group for all lower leg muscles ($p<0.05$), except for the PER muscle in the NFI DMD group ($p=0.19$)(Figure 3a). $T_2$ values were significantly increased in both the NFI and FI group in all muscles compared to healthy controls, except for the TA muscle in the NFI group (Figure 3b). In addition, intracellular tissue pH was significantly increased in the FI DMD group compared to healthy controls for all muscles ($p<0.01$), while in the NFI group the PER and TA muscle showed significantly increased pH levels. (Figure 4b) Pi/PCR was significantly elevated in the GL, SOL

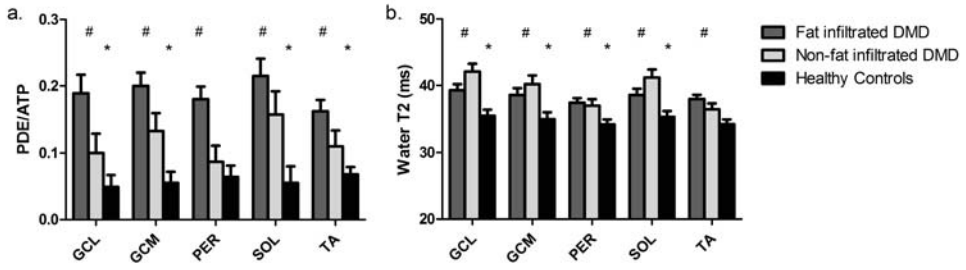


**Figure 3.** Mean values ±SD for PDE/ATP (a) and $T_2$ (b) in healthy controls (black) non-fat infiltrated DMD patients (light grey) and fat infiltrated DMD patients (dark grey) are shown per muscle. Significant differences between NFI DMD patients and controls are marked with an asterisk (*) and significant differences between FI DMD patients and controls are marked with an number sign (#). (PDE = phosphodiester, ATP=adenosine triphosphate, GL/GM= lateral and medial head gastrocnemius, PER= peroneus, SOL=soleus, TA=anterior tibialis)



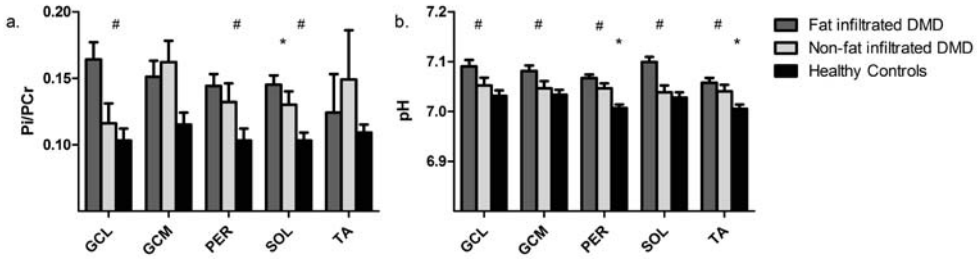


**Figure 4.** Mean values +/- SD for Pi/PCr (a) and pH (b) in healthy controls (black) non-fat infiltrated DMD patients (light grey) and fat infiltrated DMD patients (dark grey) are shown per muscle. Significant differences between NFI DMD patients and controls are marked with an asterisk (*) and significant differences between FI DMD patients and controls are marked with an number sign (#). (Pi = inorganic phosphate, PCr = phosphocreatine, GL/GM= lateral and medial head gastrocnemius, PER= peroneus, SOL=soleus, TA=anterior tibialis)

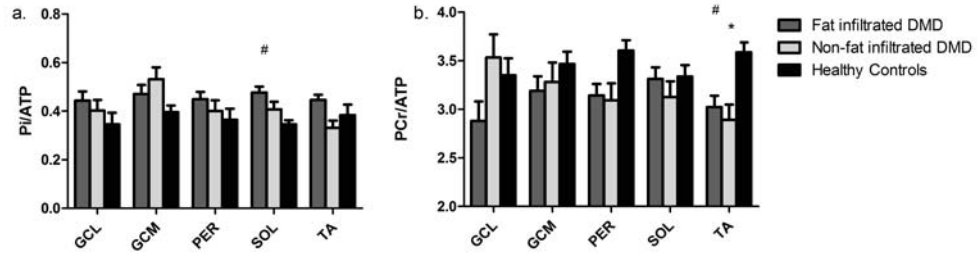


**Figure 5.** Mean values ±SD for Pi/ATP (a) and PCr/ATP (b) in healthy controls (black) non-fat infiltrated DMD patients (light grey) and fat infiltrated DMD patients (dark grey) are shown per muscle. Significant differences between NFI DMD patients and controls are marked with an asterisk (*) and significant differences between FI DMD patients and controls are marked with an number sign (#). (Pi = inorganic phosphate, PCr = phosphocreatine, ATP=adenosine triphosphate, GL/GM= lateral and medial head gastrocnemius, PER= peroneus, SOL=soleus, TA=anterior tibialis)

and PER muscle in the FI DMD group and in the SOL muscle in the NFI DMD group compared to healthy controls (Figure 4a). Pi/ATP was elevated in the SOL muscle for the FI group compared to healthy controls (Figure 5a). PCr/ATP was reduced in both the NFI and FI DMD group for the TA muscle compared to healthy controls. No changes were found for the other muscles (Figure 5b).

In the comparison of the FI groups versus the NFI group, only PDE/ATP was significantly elevated in all muscles, with exception of the SOL muscle. ($p<0.05$) In addition, $T_2$ values tended to be higher in NFI group compared to the FI group, although not significantly. ($p\geq0.074$) No consistent changes were found between NFI and FI DMD group for the other metabolites.

## Discussion

In this study we used a combination of quantitative proton MRI and localized $^{31}$P MR spectroscopy to evaluate high-energy phosphate levels and $T_2$ in DMD patients in muscles with and without fat replacement. By assessing $^{31}$P metabolites at 7 tesla, we were able to localize the metabolic changes within individual muscles. Since in DMD (and many other muscular dystrophies muscles) tissue is replaced with fat at different rates and at different time points, the muscle specific multi parametric datasets obtained allows the evaluation of these pathophysiological processes in different disease stages.

### *Metabolic changes in the absence of fat*

In DMD, it is thought that persistent inflammation due to muscle damage eventually results in replacement of muscle tissue with fat and fibrosis. [36] Consequently, indices which are sensitive to changes before fat replacement occurs are very valuable. Our results showed that PDE levels and $T_2$ values are already elevated compared to controls in muscles without increased fat levels. PDE levels have been hypothesized to reflect phospholipid membrane degradation products which in some situations proved to be reversible, while elevated $T_2$ values are attributed to changes in the extracellular and vascular spaces and are generally thought to reflect inflammation. [18, 37-39] Together these results suggest that these individual measures can reflect muscle damage prior to the more apparent structural changes. This is in accordance with previous work in DMD and BMD patients where elevated PDE levels were detected prior to structural changes. [17, 24] In addition, higher PDE/ATP levels were observed for all muscles in the FI DMD group compared to the NFI DMD group, with exception of the SOL muscle. This suggests that it might reflect the progressive

behaviour of the disease. This is in agreement with previous work which compared metabolic changes between patient groups and showed even higher PDE levels in DMD patients compared to BMD patients and DMD carriers. [19, 40] Interestingly, PDE showed to be one of the most responsive $^{31}$P indices to AVV exon skipping treatment in the forelimb of GRMD dogs, changing towards more healthy values. [41] Subsequently, the elevated $T_2$ values in the absence of fat detected here are in agreement with previous work in DMD patients, showing increased water $T_2$ levels in combination with low fat fractions in the Vastus Lateralis and Soleus muscle. [42] To monitor potential therapeutic effects, the ability to distinguish between affected and less affected muscle tissue in combination with the ability to revert back to normal values are important features of a surrogate biomarker.



In addition to the metabolic changes, $T_2$ values were lower in all muscles with fat infiltration compared to the muscles without fat infiltration, although not significantly. This phenomenon is often mentioned in the MR literature and has mainly been attributed to the increase in fibrotic tissue in later stages of the disease. [17, 43] Recent histological work confirmed the presence of connective and fibrotic fibers which gradually start to increase after the age of 6. [44] Interestingly, $T_2$ values have been shown to decrease in response to three months of corticosteroid therapy in DMD patients.[15] In combination with the natural course of $T_2$ in DMD this indicates that $T_2$ as potential outcome measure is primarily valuable in the early phases of the disease.

### *Metabolic changes in the presence of fat*

In muscles with increased fat infiltration, greater metabolic changes were present; in addition to PDE/ATP and T2 values, both Pi/PCr and intracellular tissue pH were significantly increased in majority of muscles with increased fat levels. The exact cause for the often-reported more alkaline intracellular tissue pH in muscular dystrophies is unclear. Two processes have been suggested to be involved; i.e. an altered proton sarcolemma membrane efflux mechanism due to a misbalance in $Ca^+$ and increased mitogenesis due to continuous muscle regeneration in DMD. The increase in Pi/PCr most likely is linked to elevated ADP concentrations due to poor coupling of the oxidative phosphorylation in resting muscle. [19, 22, 40] Interestingly, no consistent changes were found for Pi/ATP and PCr/ATP compared to controls. Up to now, all work in DMD found significantly reduced PCr/ATP levels and increased Pi/ATP levels. This contrast could be related to the studied DMD study populations. Most previous MR data have been obtained in older non-steroid treated DMD populations by using surface coil localization, resulting in more severely affected muscles, while here data was obtained relatively early in the disease course. [6, 17, 21, 22, 26, 40]

Almost no differences were detected between NFI and FI DMD group for Pi/PCr, Pi/ATP, PCr/ATP and pH which suggest non-progressive behaviour of these metabolic changes. This finding is partly in agreement with recently published longitudinal $^{31}$P MRS data in the arm muscles of DMD patients which showed that none of the metabolic indices changed linearly with age. [26] The fact that Pi, PCr and intracellular tissue pH are predominantly changed in the presence of fat points out that these various processes might occur simultaneously. Fat fraction reflects loss of muscle tissue whereas metabolic changes, as they are solely detected in muscle tissue, are thought to reflect the quality of the remaining muscle tissue. These simultaneous processes yield complementary information and stress the importance of assessing multiple aspects of muscle damage in both early and later stages of the disease.

Taken combined, our results provide more insight in the time relation between the various pathophysiological processes which take place in muscle; as PDE/ATP and $T_2$ are elevated in the absence of fat, these might be the first signs of damage detectable with MR. Thereafter, apparently intracellular tissue pH and Pi/PCr become altered, as they are predominantly found in muscles with fat infiltration. Simultaneously with these metabolic changes, muscle tissue is replaced by fat and fibrotic tissue which is reflected by increased fat levels compared to controls and an apparent decrease in $T_2$ values. Finally, we showed only minor changes in muscle Pi/ATP and PCr/ATP. Suggesting that these metabolites remain relatively well preserved in the early disease stages. Based on previous work it seems that in later disease stages, muscle energy metabolism becomes increasingly misbalanced after which Pi/ATP and PCr/ATP also show changes. [6, 19, 22, 26] It is highly probable that this imbalance in energy metabolism will increase until all muscle tissue is replaced by fat and fibrotic tissue.

### *Limitations*

Some limitations of the study should be acknowledged. First of all, a large number of spectra (16 out of 90) had to be discarded due to insufficient quality as a result of a low SNR in muscles with extensive fat replacement. This could have resulted in some bias in regards to the less severely affected muscles. However, as metabolic changes which were present in muscles without fat replacement were even more pronounced in muscles with fat replacement, we do not think that any changes that were present went undetected. Secondly, the identification of voxel solely in an individual muscle is somewhat complicated using a 2D-CSI sequence as the diameters of the muscle change along the length of the leg. To circumvent this problem, the anatomical images used to plan the 2D-CSI sequence were carefully checked to ensure that one voxel was located within one individual muscle over the full length of the coil prior to starting the scan. Thirdly, no $B_1^+$ correction was used for the tri-exponential T2 fitting

method applied here, which could have resulted in some bias in the determination of the $T_2$ values in areas with low $B1^+$. However, this seems to be particularly the case for the upper leg, [45] whereas due to the smaller dimensions the problem seems to be less pronounced in the lower leg. [46] Lastly, quantitative imaging datasets were acquired at 3T, while MRS data were acquired at 7T. To minimize localization errors as much as possible, the FISP sequence used for carefully positioning the 2D-CSI at the 7T was also assessed to select the corresponding slices on the 3-Point Gradient Echo Dixon and T2 MSE acquired at the 3T system.

### *Conclusion*

In conclusion, our results show that with the combination of quantitative proton MRI and localized $^{31}$P MR spectroscopy we were able to distinguish between early and late pathophysiological changes in DMD patients. Both PDE levels and T2 values are not only already changed prior to the presence of fat infiltration, but remain elevated in more severely affected muscles. This suggest that these measures could not only function as early markers for muscle damage, but could also reflect a potentially reversible pathology in more advanced stages of the disease. Future work will aim to assess spatially localized longitudinal multimodal MR measures in DMD to be able to evaluate these processes over time.

## References


1. Bushby KMD, Gardnermedwin D. The Clinical, Genetic and Dystrophin Characteristics of Becker Muscular-Dystrophy .1. Natural-History (Vol 240, Pg 98, 1993). J Neurol 1993;240:453-453.
2. Hoffman EP, Brown RH, Kunkel LM. Dystrophin - the Protein Product of the Duchenne Muscular-Dystrophy Locus. Cell 1987;51:919-928.
3. Rosenberg AS, Puig M, Nagaraju K, et al. Immune-mediated pathology in Duchenne muscular dystrophy. Sci Transl Med 2015;7.
4. Willcocks RJ, Arpan IA, Forbes SC, et al. Longitudinal measurements of MRI-T-2 in boys with Duchenne muscular dystrophy: Effects of age and disease progression. Neuromuscular Disord 2014;24:393-401.
5. Arpan I, Forbes SC, Lott DJ, et al. T-2 mapping provides multiple approaches for the characterization of muscle involvement in neuromuscular diseases: a cross-sectional study of lower leg muscles in 5-15-year-old boys with Duchenne muscular dystrophy. Nmr Biomed 2013;26:320-328.
6. Newman RJ, Bore PJ, Chan L, et al. Nuclear Magnetic-Resonance Studies of Forearm Muscle in Duchenne Dystrophy. Brit Med J 1982;284:1072-1074.
7. Fischmann A, Hafner P, Fasler S, et al. Quantitative MRI can detect subclinical disease progression in muscular dystrophy. J Neurol 2012;259:1648-1654.
8. Fischmann A, Hafner P, Gloor M, et al. Quantitative MRI and loss of free ambulation in Duchenne muscular dystrophy. J Neurol 2013;260:969-974.
9. Hollingsworth KG, Garrood P, Eagle M, Bushby K, Straub V. Magnetic Resonance Imaging in Duchenne Muscular Dystrophy: Longitudinal Assessment of Natural History over 18 Months. Muscle Nerve 2013;48:586-588.
10. Wokke BH, van den Bergen JC, Versluis MJ, et al. Quantitative MRI and strength measurements in the assessment of muscle quality in Duchenne muscular dystrophy. Neuromuscular Disord 2014;24:409-416.
11. Akima H, Lott D, Senesac C, et al. Relationships of thigh muscle contractile and non-contractile tissue with function, strength, and age in boys with Duchenne muscular dystrophy. Neuromuscular Disord 2012;22:16-25.
12. Kim HK. T2 Mapping in Duchenne Muscular Dystrophy: Distribution of Disease Activity and Correlation with Clinical Assessments (vol 255, pg 899, 2010). Radiology 2010;256:1016-1016.
13. Kim HK, Laor T, Horn PS, Wong B. Quantitative Assessment of the T2 Relaxation Time of the Gluteus Muscles in Children with Duchenne Muscular Dystrophy: a Comparative Study Before and After Steroid Treatment. Korean J Radiol 2010;11:304-311.
14. Forbes SC, Walter GA, Rooney WD, et al. Skeletal Muscles of Ambulant Children with Duchenne Muscular Dystrophy: Validation of Multicenter Study of Evaluation with MR Imaging and MR Spectroscopy. Radiology 2013;269:198-207.
15. Arpan I, Willcocks RJ, Forbes SC, et al. Examination of effects of corticosteroids on skeletal muscles of boys with DMD using MRI and MRS. Neurology 2014;83:974-980.
16. Carlier PG. Global T2 versus water T2 in NMR imaging of fatty infiltrated muscles: Different methodology, different information and different implications. Neuromuscular Disord 2014;24:390-392.
17. Wary C, Azzabou N, Giraudeau C, et al. Quantitative NMRI and NMRS identify augmented disease progression after loss of ambulation in forearms of boys with Duchenne muscular dystrophy. Nmr Biomed 2015;28:1150-1162.
18. Araujo ECA, Fromes Y, Carlier PG. New Insights on Human Skeletal Muscle Tissue Compartments Revealed by In Vivo T2 NMR Relaxometry. Biophys J 2014;106:2267-2274.
19. Kemp GJ, Taylor DJ, Dunn JF, Frostick SP, Radda GK. Cellular Energetics of Dystrophic Muscle. J Neurol Sci 1993;116:201-206.

20. Newman RJ, Radda G. Phosphorus Nuclear Magnetic-Resonance Studies in Duchenne and Becker Dystrophy. Clin Sci 1982;63:P36-P36.
21. Griffiths RD, Cady EB, Edwards RHT, Wilkie DR. Muscle Energy-Metabolism in Duchenne Dystrophy Studied by P-31-Nmr - Controlled Trials Show No Effect of Allopurinol or Ribose. Muscle Nerve 1985;8:760-767.
22. Younkin DP, Berman P, Sladky J, Chee C, Bank W, Chance B. P-31 Nmr-Studies in Duchenne Muscular-Dystrophy - Age-Related Metabolic Changes. Neurology 1987;37:165-169.
23. Wary C, Azzabou N, Zehrouni K, et al. One year follow-up of Duchenne muscle dystrophy with nuclear magnetic resonance imaging and spectroscopy indices. Neuromuscular Disord 2014;24:853-853.
24. Wokke BH, Hooijmans MT, van den Bergen JC, Webb AG, Verschuuren JJ, Kan HE. Muscle MRS detects elevated PDE/ATP ratios prior to fatty infiltration in Becker muscular dystrophy. Nmr Biomed 2014;27:1371-1377.
25. Kan HE, Klomp DWJ, Wohlgemuth M, et al. Only fat infiltrated muscles in resting lower leg of FSHD patients show disturbed energy metabolism. Nmr Biomed 2010;23:563-568.
26. Hogrel JY, Wary C, Moraux A, et al. Longitudinal functional and NMR assessment of upper limbs in Duchenne muscular dystrophy. Neurology 2016;86:1022-1030.
27. Zijnen; JCvdBHBGAJvERPIJMdGPJWMP. Forty-Five years of Duchenne muscular dystrophy in the Netherlands. Journal of Neuromuscular Diseases 2014:99-109.
28. Naressi A, Couturier C, Devos JM, et al. Java-based graphical user interface for the MRUI quantitation package. Magn Reson Mater Phy 2001;12:141-152.
29. Bogner W, Chmelik M, Schmid AI, Moser E, Trattnig S, Gruber S. Assessment of (31)P Relaxation Times in the Human Calf Muscle: A Comparison between 3 T and 7 T In Vivo. Magn Reson Med 2009;62:574-582.
30. Taylor DJ, Kemp GJ, Woods CG, Edwards JH, Radda GK. Skeletal-Muscle Bioenergetics in Myotonic-Dystrophy. J Neurol Sci 1993;116:193-200.
31. Hamilton G, Yokoo T, Bydder M, et al. In vivo characterization of the liver fat H-1 MR spectrum. Nmr Biomed 2011;24:784-790.
32. Reeder SB, Hu HH, Sirlin CB. Proton density fat-fraction: a standardized MR-based biomarker of tissue fat concentration. J Magn Reson Imaging 2012;36:1011-1014.
33. Yu HZ, Shimakawa A, McKenzie CA, Brodsky E, Brittain JH, Reeder SB. Multiecho Water-Fat Separation and Simultaneous R-2* Estimation With Multifrequency Fat Spectrum Modeling. Magn Reson Med 2008;60:1122-1134.
34. Loughran T, Higgins DM, McCallum M, Coombs A, Straub V, Hollingsworth KG. Improving Highly Accelerated Fat Fraction Measurements for Clinical Trials in Muscular Dystrophy: Origin and Quantitative Effect of R2*Changes. Radiology 2015;275:570-578.
35. Azzabou N, Loureiro de Sousa P, Caldas E, Carlier PG. Validation of a generic approach to muscle water T2 determination at 3T in fat-infiltrated skeletal muscle. J Magn Reson Imaging 2015;41:645-653.
36. Azzabou N, Carlier PG. Fat quantification and T2 measurement. Pediatr Radiol 2014;44:1620-1621.
37. Sterin M, Cohen JS, Mardor Y, Berman E, Ringel I. Levels of phospholipid metabolites in breast cancer cells treated with antimitotic drugs: A P-31-magnetic resonance spectroscopy study. Cancer Res 2001;61:7536-7543.
38. Argov Z, Maris J, Damico L. Invivo Phosphorus Nuclear Magnetic-Resonance (P-31-Nmr) Study of Dystrophic Hamster Muscle. J Neurol Sci 1988;86:185-193.
39. Damon BM, Gregory CD, Hall KL, Stark HJ, Gulani V, Dawson MJ. Intracellular acidification and volume increases explain R-2 decreases in exercising muscle. Magn Reson Med 2002;47:14-23.

40. Barbiroli B, Funicello R, Iotti S, Montagna P, Ferlini A, Zaniol P. P-31-Nmr Spectroscopy of Skeletal-Muscle in Becker Dystrophy and Dmd Bmd Carriers - Altered Rate of Phosphate-Transport. J Neurol Sci 1992;109:188-195.
41. Le Guiner C, Montus M, Servais L, et al. Forelimb Treatment in a Large Cohort of Dystrophic Dogs Supports Delivery of a Recombinant AAV for Exon Skipping in Duchenne Patients. Mol Ther 2014;22:1923-1935.
42. Forbes SC, Willcocks RJ, Triplett WT, Rooney WD, Lott DJ. Magnetic Resonance Imaging and Spectroscopy Assessment of Lower Extremity Skeletal Muscles in Boys with Duchenne Muscular Dystrophy: A Multicenter Cross Sectional Study (vol 9, e106435, 2014). Plos One 2014;9.
43. Willcocks RJ, Rooney WD, Triplett WT, et al. Multicenter prospective longitudinal study of magnetic resonance biomarkers in a large duchenne muscular dystrophy cohort. Ann Neurol 2016;79:535-547.
44. Peverelli L, Testolin S, Villa L, et al. Histologic muscular history in steroid-treated and untreated patients with Duchenne dystrophy. Neurology 2015;85:1886-1893.
45. Brink WMV, M.J. ¡Peeters, J.M. ; Boernert, P. ; Webb, A.G.; . Passive radiofrequency shimming in the thighs at 3 Tesla using high permittivity materials and body coil receive uniformity correction. Magn Reson Med 2015:00:00.
46. Hooijmans MT, Dzyubachyk O, Nehrke K, et al. Fast multistation water/fat imaging at 3T using DREAM-based RF shimming. J Magn Reson Imaging 2015;42:217-223.

## *Supplementary data*

| | Controls | NFI DMD | FI DMD |
|---|---|---|---|
| **GL** | n=12 | n= 5 | n= 7 |
| Pi/ATP | 0.35±0.05 | 0.4±0.04 | 0.44±0.04 |
| Pi/PCr | 0.1±0.01 | 0.12±0.02 | 0.16±0.01*$ |
| PCr/ATP | 3.35±0.17 | 3.5±0.2 | 2.9±0.2 |
| PDE/ATP | 0.05±0.02 | 0.1±0.03* | 0.19±0.03*$ |
| pH | 7.03±0.01 | 7.05±0.02 | 7.09±0.013* |
| T2 (ms) | 35.5±0.9 | 42.1±1.2* | 39.3±0.9* |
| Fat fraction(%) | 8.4±1.5 | 11.7±1.7 | 46.8±19.7 |
| **GM** | n=12 | n= 6 | n= 8 |
| Pi/ATP | 0.396±0.047 | 0.53±0.05 | 0.47±0.04 |
| Pi/PCr | 0.12±0.009 | 0.16±0.02 | 0.15±0.012 |
| PCr/ATP | 3.47±0.13 | 3.29±0.2 | 3.19±0.15 |
| PDE/ATP | 0.06±0.02 | 0.13±0.03* | 0.2±0.02*$ |
| pH | 7.03±0.01 | 7.05±0.02 | 7.08±0.01* |
| T2 (ms) | 34.9±1.02 | 40.2±1.3* | 38.6±1* |
| Fat fraction(%) | 7.6±1.2 | 9.7±1.1 | 50.1 ±21.8 |
| **PER** | n= 12 | n= 4 | n= 12 |
| Pi/ATP | 0.37±0.05 | 0.4±0.05 | 0.45±0.03 |
| Pi/PCr | 0.1±0.01 | 0.13±0.01 | 0.14±0.01* |
| PCr/ATP | 3.6±0.11 | 3.1±0.17 | 3.2±0.12 |
| PDE/ATP | 0.06±0.02 | 0.09±0.02 | 0.18±0.02*$ |

table continued

| | | | |
|---|---|---|---|
| pH | 7.01±0.01 | 7.05±0.01* | 7.07±0.01* |
| T2 (ms) | 34.2±0.7 | 36.9±0.97* | 37.4±0.7* |
| Fat fraction(%) | 10.2±1.2 | 12.2±0.6 | 38.7±21.2 |
| **SOL** | n= 12 | n= 7 | n= 11 |
| Pi/ATP | 0.35±0.02 | 0.41±0.03 | 0.48±0.02* |
| Pi/PCr | 0.1±0.01 | 0.13±0.01* | 0.15±0.01* |
| PCr/ATP | 3.34±0.12 | 3.13±0.16 | 3.3±0.12 |
| PDE/ATP | 0.06±0.02 | 0.16±0.04* | 0.22±0.03* |
| pH | 7.03±0.01 | 7.04±0.01 | 7.09±0.01*$ |
| T2 (ms) | 35.3±0.9 | 41.2±1.2* | 38.6±0.9* |
| Fat fraction(%) | 7.8±1.9 | 10.7±1.5 | 43.5±16.3 |
| **TA** | n= 12 | n= 7 | n= 8 |
| Pi/ATP | 0.28±0.04 | 0.33±0.03 | 0.45±0.02 |
| Pi/PCr | 0.12±0.01 | 0.15±0.04 | 0.12±0.03 |
| PCr/ATP | 3.59±0.10 | 2.9±0.16* | 3.02±0.12* |
| PDE/ATP | 0.07±0.01 | 0.11±0.02* | 0.16±0.02*$ |
| pH | 7.01±0.01 | 7.04±0.01* | 7.06±0.01* |
| T2 (ms) | 34.1±0.7 | 36.4±0.9 | 37.9±0.7* |
| Fat fraction(%) | 8.2±1.3 | 8.9±1.2 | 30.1±8.9 |

**Table 1.** Mean values ±SD for the different metabolites, T2 and %fat in healthy controls, DMD patients with no fat infiltration (NFI) and DMD patients with fat infiltration (FI). Significant differences between patients and controls are marked with an asterisk (*). Significant differences between NFI and FI DMD patients are marked with a dollar sign ($). (Pi = inorganic phosphate, PDE = phosphodiester, PCr = phosphocreatine, ATP=adenosine triphosphate GL/GM= lateral and medial head gastrocnemius, PER= peroneus, SOL=soleus, TA=anterior tibialis)